



HAL
open science

Polyethylene and poly(ethylene- co -vinyl acetate) star polymers by iodine transfer polymerization

Florian Baffie, Olivier Boyron, Muriel Lansalot, Vincent Monteil, Franck D'Agosto

► **To cite this version:**

Florian Baffie, Olivier Boyron, Muriel Lansalot, Vincent Monteil, Franck D'Agosto. Polyethylene and poly(ethylene- co -vinyl acetate) star polymers by iodine transfer polymerization. *Polymer Chemistry*, 2023, 14 (38), pp.4419-4428. 10.1039/d3py00849e . hal-04286213

HAL Id: hal-04286213

<https://hal.science/hal-04286213v1>

Submitted on 15 Nov 2023

HAL is a multi-disciplinary open access archive for the deposit and dissemination of scientific research documents, whether they are published or not. The documents may come from teaching and research institutions in France or abroad, or from public or private research centers.

L'archive ouverte pluridisciplinaire **HAL**, est destinée au dépôt et à la diffusion de documents scientifiques de niveau recherche, publiés ou non, émanant des établissements d'enseignement et de recherche français ou étrangers, des laboratoires publics ou privés.



Distributed under a Creative Commons Attribution - NonCommercial 4.0 International License



Polyethylene and poly(ethylene-co-vinyl acetate) star polymers by iodine transfer polymerization.

Florian Baffie, Olivier Boyron, Muriel Lansalot, Vincent Monteil, Franck D'Agosto*

Received 00th January 20xx,
Accepted 00th January 20xx

DOI: 10.1039/x0xx00000x

www.rsc.org/

Iodine transfer (co)polymerization (ITP) was employed to form polyethylene (PE) and poly(ethylene-co-vinyl acetate) (EVA). ITPs were conducted at 80 bar pressure of ethylene in dimethylcarbonate (DMC) at 70°C using tri- and tetra-iodofunctionalized chain transfer agents (CTAs) leading to secondary reinitiating radicals. To better comprehend their behaviour, a full study was undertaken to compare the kinetics, the structures of the final polymer and the molar mass control obtained when using analogous iodo and di-iodo CTAs leading to the same secondary reinitiating radicals. Well-defined linear PEs carrying one or two iodo chain ends could be formed together with three- and four-arm star PE. The possibility to cleave each arm of the corresponding star structures allowed to show good control of the polymerizations. The transposition to the copolymerization of ethylene and vinyl acetate led to the formation of well-defined four arm star EVA.

Introduction

Star polymers are spatially defined polymers that have attracted and still attract great interest among chemists and material scientists who take advantage of these higher-order and compact architectures to generate unique properties. The development of star polymers has been closely linked to the advances in polymerization techniques, particularly in living polymerizations.¹ Several strategies have been used to form star polymers by combining or not controlled/living polymerizations and highly efficient coupling chemistries and among them: arm-first, coupling-onto, and core-first. The arm-first strategy involves the synthesis of linear and well-defined end-functionalized polymer chains and their subsequent crosslinking.² On the other hand, in the coupling-onto strategy,³ the preformed linear end-functionalized polymer chains are attached onto a multifunctional agent by a coupling reaction.⁴ The core-first strategy employs a multifunctional initiator to form star polymers by the simultaneous growth of polymer arms by controlled/living polymerizations. Each of these strategies has both inherent advantages and disadvantages. For example, in the arm-first strategy, the number of arms is difficult to control but can be very high. In contrast, with the core-first approach, the number of arms is limited but well defined.⁵

In the particular case of polyethylene (PE), synthetic pathways to produce star polymers have relied on the anionic

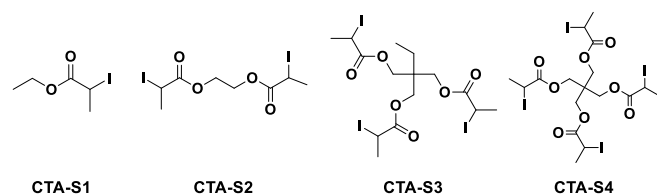
polymerization of butadiene to produce stars according to the above-mentioned strategies followed by hydrogenation.^{6, 7} Preformed PE chains functionalized with appropriate end groups have been involved in arm-first strategies.^{8, 9} Ma et al.¹⁰ originally used polyhomologation of ylides to produce polymethylenes, analogue to polyethylene, from which two polystyrene arms could be grown by reversible-deactivation radical polymerization (RDRP) to yield mikto-arm star polymers. The core-first strategy was implemented by using living ethylene coordination-insertion polymerization with a Pd complex to produce star polyethylenes. The polymerization takes advantage of the formation of a trifunctional active species by combination of the Pd complex with a triacrylate.¹¹⁻¹³ This last strategy is straightforward as the star PE is formed directly from polymerization without additional chemistry step. The living nature of the polymerization is however costly in metal (one per chain) and sensitive to polar species and potential polar comonomers.

We recently focused on strategies to produce well-defined polyethylene stars by the core-first method using exclusively RDRPs. Indeed, in the last ten years, RDRPs of ethylene were successfully achieved using techniques based on a reversible degenerative (DT) chain transfer. Among the different techniques amenable to control the free radical polymerization of ethylene by DT, reversible addition-fragmentation chain transfer (RAFT),^{14, 15} organotellurium mediated radical polymerization (TeRP)¹⁶ and iodine transfer polymerization (ITP)¹⁷ have been successfully used to control the free radical growth of the PE chains. Copolymerization with polar monomers such as vinyl acetate (VAc) was also successfully conducted with RAFT,^{14, 15, 18} ITP^{17, 19} and cobalt mediated radical polymerization (CoMRP).^{20, 21, 22} As far as we know, there

Univ Lyon, Université Claude Bernard Lyon 1, CPE Lyon, CNRS, UMR 5128, Catalysis, Polymerization, Processes and Materials (CP2M), 43 Bd du 11 Novembre 1918, 69616 Villeurbanne, France. franck.dagosto@univ-lyon1.fr
Electronic Supplementary Information (ESI) available: See DOI: 10.1039/x0xx00000x

is no example of star PE obtained by RDRP of ethylene using a core-first strategy. Besides, only one example of star copolymers based on ethylene and vinyl acetate (EVA) has been depicted by RAFT using a trifunctional chain transfer agent (CTA).¹⁸

Star polymers based on methyl methacrylate have been synthesized by ITP using multifunctional alkyl iodides as CTAs according to a core-first strategy.^{23, 24} In these studies, 3-arm star polymers were synthesized using an alkyl tri-iodide CTA. Considering the successful use of ITP to control ethylene (co)polymerization, a similar strategy was used in the present paper to investigate for the first time a core-first synthesis of star PE starting from ethylene as monomer. An EVA star polymer is also investigated. To achieve this goal, tri and tetrafunctional CTA-S3 and CTA-S4 (**Scheme 1**), respectively, were considered. Mono- and di-functional CTA-S1 and CTA-S2 (**Scheme 1**) were also considered for the sake of comparison. As part of a synthetic strategy, these CTAs have significant advantages. Their precursors are readily available and cheap. Furthermore, the ester moiety remaining at the core of the structures can be hydrolyzed to retrieve and characterize the polymer arms.



Scheme 1. Multifunctional alkyl iodides employed to mediate ITP.

Experimental

Materials

Ethylene (Air liquid, 99.95%), 2,2'-azobis(isobutyronitrile) (AIBN, Aldrich, 98%), ethyl 2-bromopropionate (Aldrich, 99%), 2-bromopropionyl bromide (Aldrich, 97%), ethylene glycol (Aldrich, > 99%), trimethylolpropane (Aldrich, 97%), pentaerythritol (Aldrich, 98%), sodium iodide (Aldrich, > 99.5%), triethylamine (Et₃N, Aldrich, > 99%), pyridine (Aldrich, > 99%), tetrahydrofuran (THF, Fisher, HPLC grade), acetone (Aldrich, > 99.5%), dichloromethane (Aldrich, > 99.5%), sodium thiosulfate (Na₂S₂O₃, Aldrich, 99%), sodium bicarbonate (NaHCO₃, Aldrich, > 99%), ammonium chloride (NH₄Cl, Aldrich, > 99.5%), magnesium sulfate (MgSO₄, Aldrich, > 99.5%), and dodecane (Aldrich, 99%) were used as received.

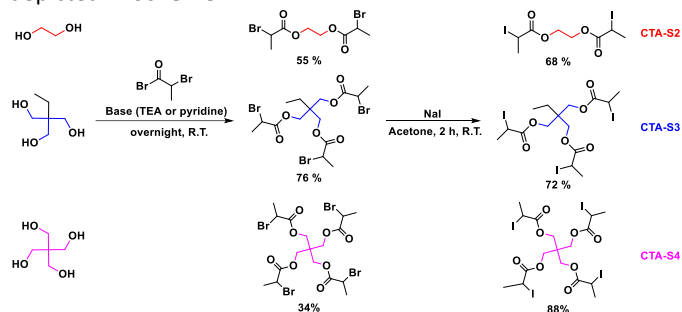
Dimethyl carbonate (DMC, Aldrich, 99%) was used after bubbling with argon for more than 12 h. Vinyl acetate (VAc, Sigma, > 99%) was purified over neutral alumina and was used after bubbling with argon for more than 12 h. Tetrachloroethylene (TCE, ACS reagent, Aldrich) was purified by passing through silica.

Methods

Synthesis of ethyl 2-iodopropionate (CTA-S1).²³ To a solution of ethyl 2-bromopropionate (10.22 g, 57.0 mmol, 1.0 eq.) in dry acetone (50 mL) was added a solution of sodium iodide (NaI, 24.90 g, 166.0 mmol, 3.0 eq.) in dry acetone (50 mL). The mixture was stirred at room temperature (R.T.) for two hours. The salts were removed by filtration and the filtrate was concentrated under reduced pressure. The crude product was dissolved in dichloromethane (80 mL), washed with a saturated solution of Na₂S₂O₃ (3 × 50 mL) and water (3 × 50 mL). The organic layer was dried over MgSO₄, filtered, concentrated *in vacuo* to afford the desired product as yellowish liquid (8.25 g, 65%).

¹H NMR (400 MHz, CDCl₃) δ (ppm) = 4.35 (q, *J* = 6.9 Hz, 1H, I-CH-CH₃), 4.28 – 4.17 (m, 2H, O-CH₂-CH₃), 1.82 (d, *J* = 6.9 Hz, 3H, I-CH-CH₃), 1.30 (t, *J* = 7.1 Hz, 3H, O-CH₂-CH₃) ¹H NMR (400 MHz, TCE+C₆D₆) δ (ppm) = 4.25 (q, *J* = 7.0 Hz, 1H, I-CH-CH₃), 4.08 – 3.91 (m, 2H, O-CH₂-CH₃), 1.76 (d, *J* = 7.0 Hz, 3H, I-CH-CH₃), 1.07 (t, *J* = 7.1 Hz, 3H, O-CH₂-CH₃) ¹³C NMR (101 MHz, CDCl₃) δ (ppm) = 172.0 (C_q, C=O), 61.9 (CH₂, O-CH₂-CH₃), 23.5 (CH, I-CH-CH₃), 13.9 (CH₃, O-CH₂-CH₃), 13.4 (CH₃, I-CH-CH₃) ¹³C NMR (101 MHz, TCE+C₆D₆) δ (ppm) = 171.0 (C_q, C=O), 61.5 (CH₂, O-CH₂-CH₃), 23.8 (CH, I-CH-CH₃), 14.0 (CH₃, O-CH₂-CH₃), 13.0 (CH₃, I-CH-CH₃) HRMS (ESI⁺): [M+H]⁺ *m/z* = 228.9720 (calc.), 228.9722 (exp.); [M+Na]⁺ *m/z* = 250.9539 (calc.), 250.9541 (exp.).

The general strategy followed for the synthesis of CTA-S2-4 is depicted in **Scheme 2**.



Scheme 2. Synthesis of CTA-S2, CTA-S3, and CTA-S4 by a two-step reaction from the corresponding alcohol precursors (% values correspond to yields).^[53,79,80]

Synthesis of ethylene glycol bis(2-iodopropionate) (CTA-S2).

Ethylene glycol (2.00 g, 32.0 mmol, 1.0 eq.) and triethylamine (22 mL, 160.0 mmol, 5.0 eq.) were dissolved in dry dichloromethane (50 mL), and the mixture was cooled to 0 °C. A solution of 2-bromopropionyl bromide (10 mL, 96.0 mmol, 3.0 eq.) in dichloromethane (50 mL) was added dropwise under argon over 20 minutes and maintained at 0 °C for an additional half an hour. The mixture was stirred at R.T. overnight. The suspension was filtered off, the solid washed with additional dichloromethane (80 mL). The filtrate was washed with water (50 mL), a saturated solution of NH₄Cl (2 × 50 mL), a saturated solution of NaHCO₃ (2 × 50 mL), and water (2 × 50 mL). The organic layer was dried over MgSO₄, filtered, concentrated *in vacuo* to afford ethylene glycol bis(2-bromopropionate) as a brown liquid (11.39 g, 55%).

^1H NMR (400 MHz, CDCl_3) δ (ppm) = 4.41 – 4.34 (m, 6H, Br-CH-CH₃ and CH₂-O), 1.79 (m, 6H, Br-CH-CH₃). ^{13}C NMR (101 MHz, CDCl_3) δ (ppm) = 170.0 (2C_q, C=O), 63.1 (2CH₂, CH₂-O), 39.7 (2CH, Br-CH-CH₃), 21.6 (2CH₃, Br-CH-CH₃). HRMS (ESI⁺): [M+Na]⁺ m/z = 352.8995 (calc.), 352.8978 (exp.).

Then, to a solution of ethylene glycol bis(2-bromopropionate) (5.00 g, 15.0 mmol, 1.0 eq.) in dry acetone (50 mL) was added a solution of sodium iodide (NaI, 6.30 g, 42.0 mmol, 2.8 eq.) in dry acetone (50 mL). The mixture was stirred at R.T. overnight. The salts were removed by filtration and the filtrate was concentrated under reduced pressure. The crude product was dissolved in dichloromethane (80 mL), washed with a saturated solution of Na₂S₂O₃ (3 × 40 mL) and water (2 × 40 mL). The organic layer was dried over MgSO₄, filtered, concentrated *in vacuo* to afford the desired product as a brown liquid (3.40 g, 65%).

^1H NMR (400 MHz, CDCl_3) δ (ppm) = 4.48 (q, J = 7.0 Hz, 2H, I-CH-CH₃), 4.43 – 4.23 (m, 4H, CH₂-O), 1.95 (d, J = 7.0 Hz, 6H, I-CH-CH₃). ^1H NMR (400 MHz, TCE+C₆D₆) δ (ppm) = 4.27 (q, J = 7.0 Hz, 2H, I-CH-CH₃), 4.07 – 4.17 (m, 6H, CH₂-O), 1.77 (d, J = 7.0 Hz, 6H, I-CH-CH₃). ^{13}C NMR (101 MHz, CDCl_3) δ (ppm) = 171.8 (2C_q, C=O), 63.0 (2CH₂, CH₂-O), 23.4 (2CH₃, I-CH-CH₃), 12.4 (2CH, I-CH-CH₃). ^{13}C NMR (101 MHz, TCE+C₆D₆) δ (ppm) = 171.0 (2C_q, C=O), 63.1 (2CH₂, CH₂-O), 23.7 (2CH₃, I-CH-CH₃), 12.1 (2CH, I-CH-CH₃). HRMS (ESI⁺): [M+Na]⁺ m/z = 448.9717 (calc.), 448.8733 (exp.).

Synthesis of trimethylolpropane tris(2-iodopropionate) (CTA-S3).²⁵ Trimethylolpropane (6.75 g, 50.0 mmol, 1.0 eq.) and triethylamine (26 mL, 190.0 mmol, 3.7 eq.) were dissolved in dry THF (150 mL), and the mixture was cooled to 0 °C. The 2-bromopropionyl bromide (19 mL, 180.0 mmol, 3.6 eq.) was added dropwise under argon over 20 minutes and maintained at 0 °C for an additional half an hour. The mixture was stirred at R.T. overnight. The suspension was filtered off, the solid washed with additional THF (80 mL) and the filtrate was concentrated under reduced pressure. The crude product was dissolved in dichloromethane (50 mL), washed with a 5% solution of Na₂SO₃ (3 × 50 mL), a saturated solution of NaHCO₃ (3 × 50 mL), and water (3 × 50 mL). The organic layer was dried over MgSO₄, filtered, concentrated *in vacuo* to afford trimethylolpropane tris(2-bromopropionate) as a yellow oil (20.75 g, 76%).

^1H NMR (300 MHz, CDCl_3) δ (ppm) = 4.37 (q, J = 7.0 Hz, 3H, Br-CH-CH₃), 4.27 – 4.01 (m, 2H, C-CH₂-O), 1.81 (d, J = 7.0 Hz, 9H, Br-CH-CH₃), 1.56 (q, J = 7.6 Hz, 2H, CH₂-CH₃), 0.92 (t, J = 7.6 Hz, 3H, CH₂-CH₃). ^{13}C NMR (101 MHz, CDCl_3) δ (ppm) = 169.8 (3C_q, C=O), 64.9 (3CH₂, C-CH₂-O), 41.7 (C_q, C-CH₂-O), 39.7 (3CH, Br-CH-CH₃), 23.0 (CH₂, CH₂-CH₃), 21.6 (3CH₃, Br-CH-CH₃), 7.5 (CH₃, CH₂-CH₃). HRMS (ESI⁺): [M+H]⁺ m/z = 558.8950 (calc.), 558.8937 (exp.).

Then, to a solution of trimethylolpropane tris(2-bromopropionate) (6.99 g, 13.0 mmol, 1.0 eq.) in dry acetone (100 mL) was added a solution of sodium iodide (NaI, 8.36 g, 55.7 mmol, 4.3 eq.) in dry acetone (50 mL). The mixture was stirred at R.T. overnight. The salts were removed by filtration and the filtrate was concentrated under reduced pressure. The crude product was dissolved in dichloromethane (80 mL), washed with a saturated solution of Na₂S₂O₃ (3 × 50 mL) and water (3 × 20 mL). The organic layer was dried over MgSO₄,

filtered, concentrated *in vacuo* to afford the desired product as an orange oil (6.36 g, 72%).

^1H NMR (400 MHz, CDCl_3) δ (ppm) = 4.50 (q, J = 7.0 Hz, 3H, I-CH-CH₃), 4.29 – 3.98 (m, 6H, C-CH₂-O), 1.96 (d, J = 7.0 Hz, 9H, I-CH-CH₃), 1.59 (q, J = 7.6 Hz, 2H, CH₂-CH₃), 0.94 (t, J = 7.6 Hz, 3H, CH₂-CH₃). ^1H NMR (400 MHz, TCE+C₆D₆) δ (ppm) = 4.27 (q, J = 7.1 Hz, 3H, I-CH-CH₃), 4.16 – 3.90 (m, 6H, C-CH₂-O), 1.77 (d, J = 7.1 Hz, 9H, I-CH-CH₃), 1.46 (q, J = 7.6 Hz, 2H, CH₂-CH₃), 0.81 (t, J = 7.6 Hz, 3H, CH₂-CH₃). ^{13}C NMR (101 MHz, CDCl_3) δ (ppm) = 171.5 (3C_q, C=O), 64.8 (3CH₂, C-CH₂-O), 41.9 (C_q, C-CH₂-O), 23.1 (3CH₃, I-CH-CH₃), 23.0 (CH₂, CH₂-CH₃), 12.4 (3CH, I-CH-CH₃), 7.6 (CH₃, CH₂-CH₃). ^{13}C NMR (101 MHz, TCE+C₆D₆) δ (ppm) = 170.7 (3C_q, C=O), 65.3 (3CH₂, C-CH₂-O), 42.6 (C_q, C-CH₂-O), 23.9 (CH₂, CH₂-CH₃), 23.8 (3CH₃, I-CH-CH₃), 12.3 (3CH, I-CH-CH₃), 7.7 (CH₃, CH₂-CH₃). HRMS (ESI⁺): [M+H]⁺ m/z = 680.8703 (calc.), 680.8702 (exp.); [M+Na]⁺ m/z = 702.8521 (calc.), 702.8521 (exp.).

Synthesis of pentaerythritol tetrakis(2-iodopropionate) (CTA-S4).²⁶ Pentaerythritol (3.00 g, 22.0 mmol, 1.0 eq.) and pyridine (13 mL, 165.0 mmol, 7.5 eq.) were dissolved in dichloromethane (60 mL) and the mixture was cooled to 0 °C. The 2-bromopropionyl bromide (49 mL, 110.0 mmol, 5.0 eq.) was added dropwise under argon over 20 minutes and maintained at 0 °C for an additional half an hour. The mixture was stirred at R.T. overnight. The suspension was filtered off, the solid was washed with additional dichloromethane (20 mL). The filtrate was washed with a saturated solution of NH₄Cl (4 × 50 mL), a saturated solution of NaHCO₃ (4 × 50 mL), and water (3 × 50 mL). The organic layer was dried over MgSO₄, filtered, concentrated *in vacuo* to afford pentaerythritol tetrakis(2-bromopropionate) as a white powder (5.02 g, 35%).

^1H NMR (400 MHz, CDCl_3) δ (ppm) = 4.39 (q, J = 6.9 Hz, 4H, Br-CH-CH₃), 4.36 – 4.18 (m, 8H, C-CH₂-O), 1.83 (d, J = 6.9 Hz, 12H, Br-CH-CH₃). ^{13}C NMR (101 MHz, CDCl_3) δ (ppm) = 169.6 (4C_q, C=O), 63.1 (4CH₂, C-CH₂-O), 43.3 (C_q, C-CH₂-O), 39.5 (4CH, Br-CH-CH₃), 21.6 (4CH₃, Br-CH-CH₃). HRMS (ESI⁺): [M+H]⁺ m/z = 671.8205 (calc.), 671.8202 (exp.).

Then, to a solution of pentaerythritol tetrakis(2-bromopropionate) (3.00 g, 4.4 mmol, 1.0 eq.) in dry acetone (50 mL) was added a solution of sodium iodide (NaI, 5.32 g, 35.5 mmol, 8.0 eq.) in dry acetone (50 mL). The mixture was stirred at R.T. overnight. The salts were removed by filtration, and the solid was washed with dry acetone (40 mL). The filtrate was concentrated under reduced pressure. The crude product was dissolved in dichloromethane (80 mL), washed with a saturated solution of Na₂S₂O₃ (3 × 50 mL) and water (2 × 20 mL). The organic layer was dried over MgSO₄, filtered, concentrated *in vacuo* to afford the desired product as an orange oil (3.33 g, 88%).

^1H NMR (400 MHz, CDCl_3) δ (ppm) = 4.52 (d, J = 7.0 Hz, 4H, I-CH-CH₃), 4.43 – 4.12 (m, 8H, C-CH₂-O), 1.97 (d, J = 7.0 Hz, 12H, I-CH-CH₃). ^1H NMR (400 MHz, TCE+C₆D₆) δ (ppm) = 4.27 (q, J = 7.0 Hz, 4H, I-CH-CH₃), 4.22 – 4.07 (m, 8H, C-CH₂-O), 1.78 (d, J = 7.0 Hz, 12H, I-CH-CH₃). ^{13}C NMR (101 MHz, CDCl_3) δ (ppm) = 171.3 (4C_q, C=O), 63.1 (4CH₂, C-CH₂-O), 43.5 (C_q, C-CH₂-O), 23.3 (4CH₃, I-CH-CH₃), 12.0 (4CH, I-CH-CH₃). ^{13}C NMR (101 MHz, TCE+C₆D₆) δ (ppm) = 170.6 (4C_q, C=O), 63.6 (4CH₂, C-CH₂-O), 44.3 (C_q, C-CH₂-O), 23.7 (4CH₃, I-CH-

C_3H_3), 11.9 (4CH, I-CH-CH₃). HRMS (ESI⁺) [M+Na]⁺ m/z = 886.7542 (calc.), 886.7545 (exp.).

Homopolymerization of ethylene. The employed stainless-steel reactor (160 mL, from Parr Instrument Co.) was equipped with a mechanical stirring apparatus, a thermometer, a pressure sensor and safety valves. A solution of CTA and AIBN (50 mg, 0.30 mmol, 6.09 mmol L⁻¹) in DMC (50 mL) was introduced through a cannula into an injecting chamber. The chamber was then pressurized at 20 bar of ethylene and opened into the preheated autoclave with a stirring speed of 600 rpm. Immediately after, ethylene gas was introduced into the reactor until a pressure of 80 bar was reached, which took about 4 min. To manage polymerization safely over 50 bar of ethylene, we used a 1.5 L intermediate tank. The tank was cooled down to -20 °C to liquefy ethylene at 40 bar. When thermodynamic equilibrium was reached, the intermediate tank was isolated and heated to reach 80 bar. This tank was used to charge the reactor and to maintain a constant pressure of ethylene in the reactor by successive manual ethylene additions. Sampling was not possible and kinetics study is achieved by performing multiple experiments for different polymerization times. After the desired time at 70 °C, the stirring was slowed down, and the autoclave was cooled with iced water. When the temperature inside the autoclave dropped below 25 °C, the remaining pressure was carefully released. The content of the reactor was collected with toluene. The evaporation of the solvent gave the polymer product.

A reference experiment (radical polymerization, RP) was also conducted in absence of CTA under the exact same conditions for the sake of comparison.

Copolymerization of ethylene and vinyl acetate. In a typical polymerization procedure, a DMC solution containing vinyl acetate, CTA and AIBN was prepared, such that the total volume was kept to 50 mL. The rest of the procedure remained the same as for ethylene homopolymerization except from the temperature and the solvent to recover the polymer which are here 70 °C and acetone, respectively.

Hydrolysis of PEs. The PEs (250 mg) obtained after 6 hours of polymerization were hydrolyzed with *t*BuOK. They were first dissolved in 25 mL of toluene at 90 °C. Then, a solution of *t*BuOK (2 M in THF, 10 equivalent per PE arm) was added, and the reaction medium was stirred at 110 °C for 4 h. The solution was then poured in 150 mL of methanol, and a white solid precipitated. The solid was filtered and dried under vacuum to afford a white powder.

Characterization

Nuclear magnetic resonance (NMR). All NMR experiments were performed at 90 °C in 2:1 TCE/deuterated benzene (C₆D₆) solutions using a Bruker Avance 400 spectrometer (¹H: 400.13 MHz; ¹³C: 100.61 MHz). The temperature was calibrated with a tube containing 80 vol% of ethylene glycol and 20 vol% of DMSO-*d*₆. ¹H NMR spectra were recorded with a 5 mm BBFO+ probe with a z-gradient coil ($D_1 = 3$ s, scans = 256, RO = 20 Hz with $O_1P = 6.5$ and $O_2P = 4.5$). Carbon NMR spectra were recorded with a 10 mm SEX probe, ¹³C selective with a z-

gradient coil. The pulse sequence used includes a decoupling proton with NOE effects, and a 70° spin excitation ($D_1 = 2$ s, scans = 6144, $O_1P = 110$ ppm, $O_2P = 80$ ppm, RO = 20 Hz). The method is said to be "semiquantitative," and the NMR calculations were carried out between carbons of the same nature (the -CH₂-). Chemical shifts are given in parts per million (ppm) with the solvent peak as internal standard.

Size exclusion chromatography (SEC). For THF insoluble polymer samples, molar mass measurements were performed using a Viscotek High-Temperature SEC (HT-SEC) system (Malvern Panalytical) that incorporates a differential refractive index detector, a viscometer, and a light scattering detector. 1,2,4-trichlorobenzene (TCB) was used as the mobile phase at a flow rate of 1 mL min⁻¹. TCB was stabilized with 2,6-di(tert-butyl)-4-methylphenol. The separation was carried out on three mixed bed columns (PLgel Olexis 300 × 7.8 mm from Malvern Instrument) and a guard column (75 × 7.5 mm). Columns and detectors were maintained at 150 °C. Sample volumes of 200 μL with concentration of 3 mg mL⁻¹ were injected and filtered online. The Omniseq software was used for data acquisition and data analysis. The molar mass distribution, number average molar mass (M_n) and dispersity (\bar{D}) were determined by means of a conventional calibration curve based on linear polyethylene standards from 300 to 130 000 g mol⁻¹ (Polymer Standards Service).

For THF soluble polymer samples, molar mass measurements were performed using a Viscotek TDA SEC (Malvern Panalytical), including a differential refractive index detector, a viscometer, a light scattering detector and a UV detector. Stabilized THF was used as the mobile phase at a flow rate of 1 mL min⁻¹ at 35 °C. All samples were injected at a concentration of 3 to 6 mg mL⁻¹ after filtration through a 0.45 μm PTFE membrane. The separation was carried out on three Agilent mixed C columns (SDVB, 5 μm, 300 × 7.5 mm) and a guard column. M_n and \bar{D} were determined by means of a conventional calibration curve or by a universal calibration based on certified PS standards (Polymer Standards Service) from 470 to 270 000 g mol⁻¹. The molar mass of an unknown PE sample of mass M is calculated based on the measurement of the intrinsic viscosity $[\eta]$, and the column retention volume, from which the product $[\eta].M$ is read on the universal calibration curve constructed with the known PS standards. Knowing independently $[\eta].M$ and $[\eta]$ leads to the calculation of M of the unknown samples. The Omniseq software was used for data acquisition and data analysis.

Gas chromatography (GC) analyses were conducted on an Agilent GC instrument 6890 equipped with a flame ionization detector (FID) and an Agilent HP-5 column (30 m × 320 μm × 0.25 μm). Injector and detector temperatures were set to 250 °C. The initial and final column temperatures were respectively 40 °C and 250 °C, with a heating rate of 20 °C min⁻¹ and a final isotherm of 2 min at 250 °C. The internal standard used was dodecane.

Mass spectrometry (MS). Mass spectrometry analyses were carried out at the *Centre commun de spectrométrie de masse* (CCSM) under the authority of the *Institut de Chimie et Biochimie Moléculaires et Supramoléculaires* (ICBMS UMR 5246, Université Claude Bernard Lyon 1, France). High-

resolution mass spectra were recorded on a Bruker MicroTOF-Q II spectrometer coupled with liquid chromatography (Agilent 1200 chain), Q-TOF analyzer (resolution: 17,500 - Mass range: 50 to 20,000), and ionization source (Electrospray (ESI)).

Differential scanning calorimetry (DSC). DSC analyses were performed on a Mettler Toledo DSC 3 equipped with 120 thermocouple sensors. An indium standard was run for calibration of the temperature and heat flow of the device. All samples were precisely weighed (ca 10 mg) and sealed in aluminium pans. Measurements were carried by two successive heating and cooling cycles (10 °C min⁻¹) with temperatures ranging from - 80 to + 150 °C. The melting and glass transition temperatures (T_m and T_g , respectively) were recorded on the second cycle. Crystallinity was calculated from the second heating curve using the following equation:

$$X_c (\%) = \left(\frac{\Delta H_m}{\Delta H_m^0} \right) \times 100$$

with $\Delta H_m^0 = 293 \text{ J g}^{-1}$ as standard enthalpy of polyethylene.

Dry nitrogen with a flow rate set at 30 mL min⁻¹ was used as purged gas.

Results and discussion

ITP of ethylene mediated by CTA-S1. Before tackling the synthesis of star polymers, we first investigated if a secondary alkyl iodide carrying an ester group is an effective CTA for ethylene polymerization. Indeed, in our seminal works, mainly fluorinated CTAs such as C₆F₁₃I^{17, 19} were studied and shown to be efficient controlling agents in ITP of ethylene.

CTA-S1-mediated ethylene polymerization was performed under conditions previously used for C₆F₁₃I^{17, 19} (70 °C, 80 bar, 50 mL of DMC, 50 mg of AIBN, and [CTA]:[AIBN] = 3:1) and compared to the exact same experiment conducted either in presence of C₆F₁₃I or in absence of CTA (free radical polymerization, RP). **Figure 1a** shows the CTA conversion and ethylene consumption *versus* polymerization time. As already observed for C₆F₁₃I,^{17, 19} no rate retardation was observed in presence of CTA-S1 compared to the RP. As C₆F₁₃I, CTA-S1 is consumed rapidly (conversion > 97% after 5 minutes) and the ethylene consumptions are comparable to those obtained with C₆F₁₃I.

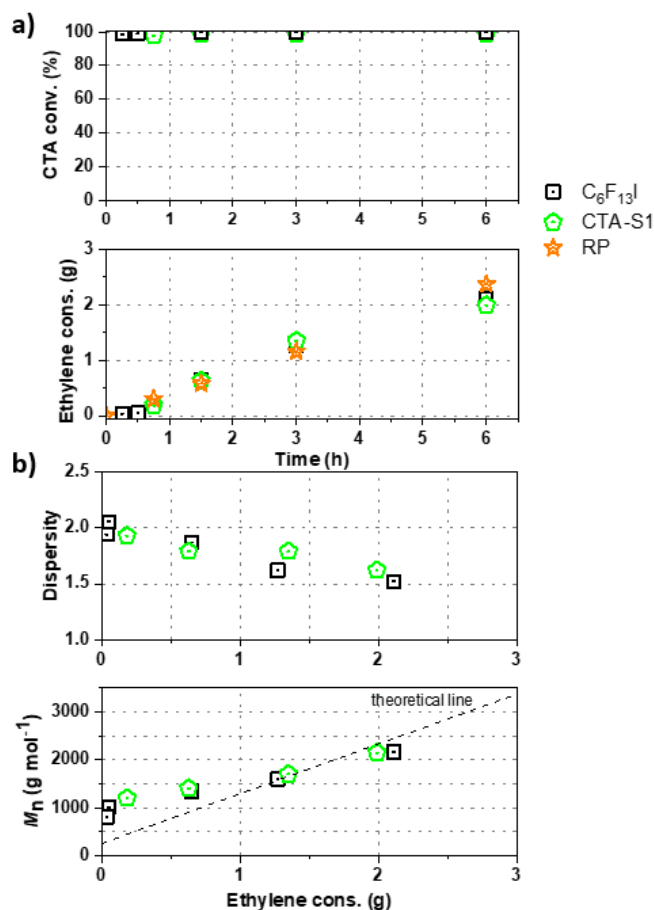


Figure 1. Polymerization conditions: T = 70 °C, P = 80 bar, [CTA]:[AIBN] = 3:1. Ethylene consumption = (mass of dried product) - (mass of AIBN) - (mass of CTA). a) Ethylene consumption and CTA conversion *versus* polymerization time for ITP systems compared to the radical polymerization (RP) performed without CTA, and b) corresponding molar mass evolutions (from HT-SEC). The radical polymerization yielded PE with M_n values of about 8000 g mol⁻¹ and \mathcal{D} values between 1.5 and 2.1. Molar masses are determined using a conventional PE calibration.

The molar mass evolution *versus* ethylene consumption is presented in **Figure 1b** and the corresponding molar mass distributions for CTA-S1 are given in Figure S1 (supporting information). The polymerization behaviour with CTA-S1 is very similar to the one with C₆F₁₃I with dispersities decreasing upon polymerization to reach values between 1.5 and 1.8 for higher molar masses. In agreement with the theory of RDRP, number average molar masses obtained by HT-SEC (M_n) are relatively close to the theory and follow the expected linear trend.

Figure 2 shows the ¹H NMR spectrum of a PE produced in the presence of CTA-S1 after 3 hours of polymerization. The iodine end-capped PE structure is shown by signal of the methylene hydrogens adjacent to the iodine atom (*a*, -CH₂I at 2.95 ppm). The use of CTA-S1 offers the possibility to see both chain-ends (*d*, -OC(=O)CH(CH₃)- at 2.30 ppm and *f*, CH₃CH₂OC(=O)- at 4.00 ppm). A comparison of signal integration from the methylene hydrogens *a* with the one of signal *f* indicates a quantitative chain-end functionality. A comparison of the signal integration from the methylene protons *a* with that of signal *f* indicates a quantitative chain-end functionality. Nevertheless, it is worth mentioning that in systems governed by reversible transfer and

conducted in the presence of azoinitiator, a fraction of dead chains corresponding at least to the fraction of chains initiated by the free radical initiator should form. In the present case, despite the rather low CTA/AIBN ratio, this fraction of chains seems minimal. The unexpected very high chain end fidelity can be related to an error associated with the determination by NMR of the integration values, although this error should remain low. This can also be due to a different decomposition rate of AIBN and initiating efficiency under high pressure (80 bar) and the conditions employed here. A good match between experimental and expected M_n values was observed after 6 hours ($M_n(\text{NMR}) = 2500 \text{ g mol}^{-1}$ vs $M_n(\text{theo.}) = 2350 \text{ g mol}^{-1}$). The discrepancy after 45 minutes ($M_n(\text{NMR}) = 950 \text{ g mol}^{-1}$ vs $M_n(\text{theo.}) = 500 \text{ g mol}^{-1}$) is probably due to the larger dispersities obtained (> 2) at the beginning of the polymerization and the transition between the pre-equilibrium and the main equilibrium governed by the reversible DT.¹⁷ These data nevertheless illustrate well the successful ITP of ethylene mediated by CTA-S1.

Besides, when setting the integral of the methylene hydrogens adjacent to the iodine chain-end to 2, the multiplet from proton *d* at 2.30 ppm shows an integral around half of the expected value (0.6 instead of 1). This is surprising as the integrals of *a* and *f* are very nicely matching. The integral value of *d* is stable throughout the polymerization, thus ruling out the possibility of H-abstraction of hydrogen *d* during polymerization. A quantitative ¹H NMR analysis with a D_1 of 50 s (instead of 3 s used routinely) was performed to ensure that protons have relaxed fully between pulses. However, the integral value of *d* remained the same. The influence of temperature analysis was also studied (70, 90 °C in TCE/C₆D₆ and 110 °C in *o*-Dichlorobenzene (DCB)/*d*-DCB) without significantly impacting the values of the corresponding integrals. The presence of an asymmetric carbon at the α chain-end ($-\text{OC}(=\text{O})\text{CH}(\text{CH}_3)\text{CH}_2-$) led us to consider whether the integral difference was not due to the presence of diastereoisomers. Indeed, the methylene hydrogens *c* ($-\text{OC}(=\text{O})\text{CH}(\text{CH}_3)\text{CH}_2-$) are diastereotopic, and the corresponding two protons are non-equivalent. This is shown by the presence of two resonances at 1.60 and 1.40 ppm for the corresponding methylene (Figure 2).^{27, 28} Therefore, we assumed that the proton *d* could also be split into two resonances, one at 2.30 ppm and the other between 1.50 and 1.75 ppm. The integrals between 1.50 and 1.75 ppm are indeed consistent with this assumption: $2H_b + 1H_c + 0.5H_d = 3.5H$. Such peculiar behavior for similar protons *d* in a poly(vinylidene fluoride) chain has indeed been already observed.²⁹

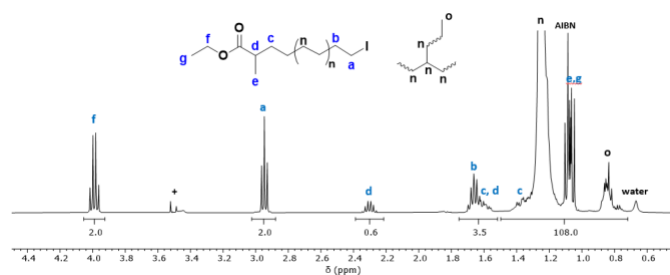


Figure 2. ¹H NMR spectrum (in TCE/C₆D₆ at 90 °C) of the PE synthesized at 70 °C, 80 bar in the presence of CTA-S1 after 3 h. + NMR solvent impurities. AIBN stands for the methyls from the chain-ends of the PE chains initiated by AIBN. The water is coming from the NMR solvent.

ITP of ethylene mediated by CTA-S2-4. With the previous good understanding of the behaviour of CTA-S1 in the control of ITP of ethylene, we then investigated the use of the three multifunctional alkyl iodides, CTA-S2-4.

Figure 3 shows the ethylene consumption *versus* polymerization time for the respective systems. Again, there is no rate retardation compared to the system without CTA. Like CTA-S1, CTA-S2-4 were consumed almost instantly.

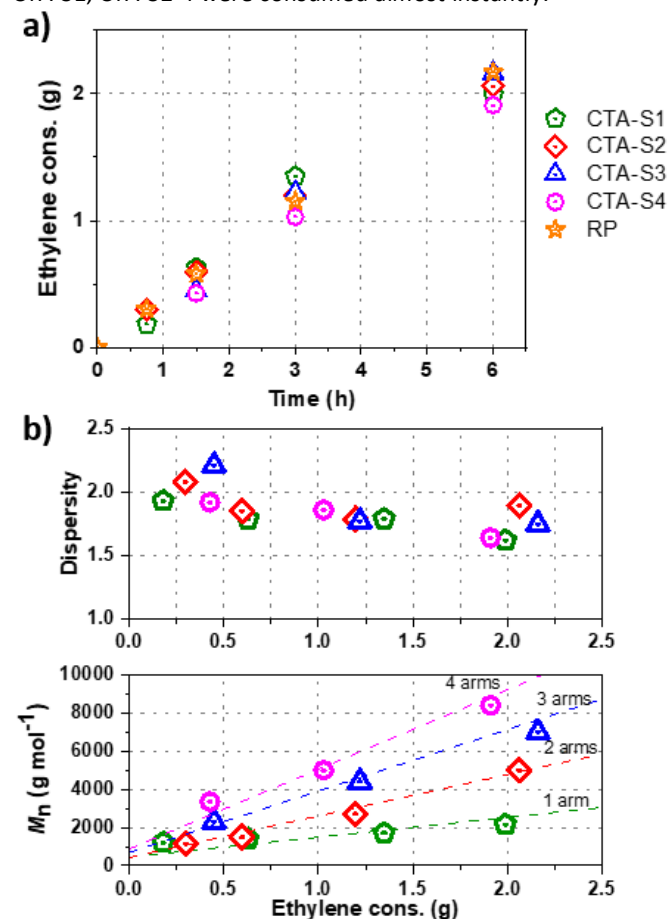


Figure 3. Polymerization conditions: T = 70 °C, P = 80 bar, [iodine]:[AIBN] = 3:1. Ethylene consumption = (mass of dried product) - (mass of AIBN) - (mass of CTA). a) Ethylene consumption *versus* polymerization time for ITP systems compared to the radical polymerization (RP) performed without CTA, and b) corresponding molar mass evolutions (from HT-SEC). Molar masses are determined by a conventional PE calibration for CTA-S1, CTA-S2 and by a universal calibration based on PS calibration for CTA-S3 and CTA-S4.

The molar mass evolution *versus* ethylene consumption is presented in **Figure 3b**, and the corresponding molar mass distributions are given in **Figure 4**. A PE calibration was used for the linear PE (CTA-S1, CTA-S2), whereas a universal calibration based on PS samples was preferred for the star polymers (CTA-S3 and CTA-S4). Molar mass distributions remain narrow, and a clear shift is observed toward higher M_n with time, indicating a successful polymerization control. As previously observed,

dispersities decrease with time to reach values between 1.6 and 1.9 for higher molar masses. M_n (HT-SEC) remained relatively close to the theory and followed the targeted linear trend (Figure 3b).

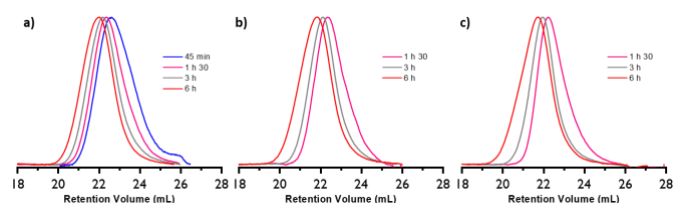


Figure 4. Molar mass distributions of PE obtained by HT-SEC during ITP of ethylene mediated by a) CTA-S2, b) CTA-S3, and c) CTA-S4 at 70 °C and 80 bar of ethylene pressure and after the indicated polymerization times.

Figure 5 shows the spectra of CTA-S4 and of the PE produced in the presence of CTA-S4 after 1.5 h and 6 h of polymerization. The characteristic resonances of CTA-S4 (d' , $-\text{OC}(=\text{O})\text{CH}(\text{CH}_3)\text{I}$ at 4.25 ppm and e' , $-\text{OC}(=\text{O})\text{CH}(\text{CH}_3)\text{I}$ at 1.80 ppm), disappear upon ethylene polymerization (Figure 5a and b). The iodine end-capped PE structure is proven by the presence of methylene hydrogens adjacent to the iodine atom (a , $-\text{CH}_2\text{I}$ at 2.95 ppm). As for CTA-S1, the use of CTA-S4 offers the possibility to see both extremities of the PE arms (f , $-\text{CH}_2\text{OC}(=\text{O})-$ at 4.10 ppm and d , $-\text{OC}(=\text{O})\text{CH}(\text{CH}_3)-$ at 2.35 ppm). A comparison of signal intensity from the methylene hydrogens a and f indicates only a minimal loss of iodine chain-end functionality (< 5%) (Figure 5c). A good match between M_n (NMR) and M_n (theo.) was observed (Figure S2). For example, after 6 hours, M_n (NMR) = 8950 g mol⁻¹ vs M_n (theo.) = 9050 g mol⁻¹. This illustrates the successful ITP of ethylene mediated by CTA-S4.

Comparably to what was observed with CTA-S1, the multiplet from proton d at 2.35 ppm presents an integral around half of the expected value (2 instead of 4) (Figure 5c). And as observed for CTA-S1, the integral of proton d is stable throughout the polymerization. Considering the very good agreement between integrals of protons a and f , consistent with successful control of the growth of 4 PE arms from CTA-S4, we again assigned this lower integral value to the effect of the diastereotopic protons of the adjacent methylene discussed in the case of CTA-S1.

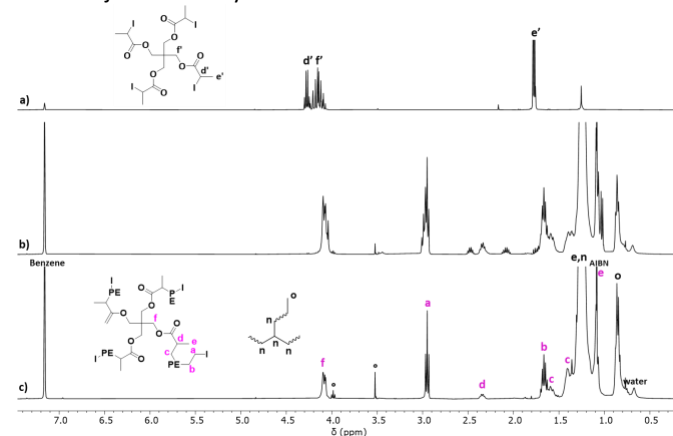


Figure 5. ¹H NMR spectra (in TCE/C₆D₆ at 90 °C) of a) CTA-S4, and PE synthesized in the presence of CTA-S4 after b) 1.5 h and c) 3 h. The end group $-\text{CH}_3$ stems from

intramolecular and intermolecular chain transfer inherent in ethylene radical polymerization. α transfer to polymerization solvent DMC. AIBN stands for the methyls from the chain-ends of the PE chains initiated by AIBN. The water is coming from the NMR solvent.

¹H NMR analyses of PEs synthesized in the presence of CTA-S2, CTA-S3 and CTA-S4 exhibit the same features and led to very similar behaviour and conclusions (see Figure S2 in Supporting information).

Moreover, two multiplets of small intensity at 2.05 and 2.45 ppm can be observed at short polymerization times in each case (Figure 5b, after 1h30 for CTA-S4). The resonances of the protons a at 2.95 ppm are also superimposed with other triplets. Their intensities decrease over time, and they disappear after 6 hours of polymerization (Figure 5c).

To elucidate the origin of these signals, the copolymer obtained after 1h30 in the presence of CTA-S4 was purified by precipitation in methanol. The polymer (200 mg) was dissolved in 20 mL of toluene at 90 °C and stirred for two hours. The solution was subsequently poured in 150 mL of methanol, and a white solid precipitated. The solid was filtered and dried under vacuum to afford a white powder (175 mg). After evaporation of the filtrate, a white wax was obtained (25 mg). The solid (Figure 6c) and the filtrate residue (Figure 6b) were analyzed by ¹H NMR. The two multiplets at 2.05 and 2.45 ppm are no longer visible in the solid obtained from precipitation, confirming that these resonances are impurities of low molar mass. On the other hand, these signals are more intense in the filtrate residue. These observations are very similar and consistent with the ones made when synthesizing telechelic PEs using fluorinated di-iodo CTA.¹⁹ In this case, the origin of these signals arose from (i) the formation of asymmetric oligomers during the degenerative chain transfer preequilibrium, and (ii) the impact of the first additions of ethylene units on the chemical shifts of the protons of the α - and ω -chain ends in the formed products. In the present case, the same explanation can be given. The disappearance of the signals at 2.05 and 2.45 ppm and the very clean triplet for proton a obtained after 6 hours of polymerization (Figure 6c) shows that the PE arms are indeed growing on all the branches of the targeted star.

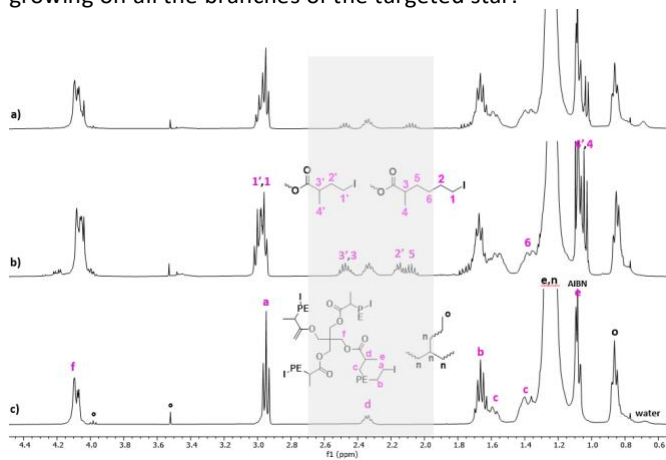


Figure 6. ¹H NMR spectra (in TCE/C₆D₆ at 90 °C) of PE synthesized at 70 °C, 80 bar in the presence of CTA-S4 after 1h30, a) before reprecipitation, and after precipitation: b) after evaporation of the filtrate and c) solid part. The end group $-\text{CH}_3$ stems from

intramolecular and intermolecular chain transfer inherent in ethylene radical polymerization. AIBN stands for the methyls from the chain-ends of the PE chains initiated by AIBN. The water is coming from the NMR solvent.

Characterization of the star structure in CTA-S3-4-mediated ITP of ethylene. In the following, we used SEC analyses and degradation reactions to prove that the expected three and four-arm star PE structures were obtained with CTA-S3 and CTA-S4, respectively.

SEC separates the chains in a polymer sample based on their hydrodynamic sizes (radius of gyration, R_g). A branched polymer and its analogue linear polymer of equal R_g elute thus out at the same rate. Therefore, SEC cannot differentiate both polymers. For the same molar mass, the R_g of a linear polymer is higher than the one of a branched polymer.³⁰ The branching content can be obtained from either the viscometer or the light scattering detector. However, the molar masses of the PE used in this study are too low to consider measurement with a light scattering detector (isotropic scattering).³⁰⁻³²

Zimm and Stockmayer proposed different formulae to calculate the number of arms in a polymer, depending on the architecture (well-defined star, brush, comb). For polymers with branches randomly distributed, the number of branches (B_n) is correlated to the branching factor (g) (Equation 1).³³

$$g = \frac{6}{2B_n} \left(\frac{2+B_n^{0.5}}{B_n} \ln \left(\frac{(2+B_n)^{0.5} + B_n^{0.5}}{(2+B_n)^{0.5} - B_n^{0.5}} \right) - 1 \right) \quad (1)$$

In the case of a well-defined star, it can be simplified to give Equation 2.

$$g = \frac{6B_n}{(B_n+1)(B_n+2)} \quad (2)$$

The branching factor g can be expressed with the viscosity branching factor (g') and the structure factor (ϵ) (Equation 3).³⁴

$$g' = g^\epsilon \quad (3)$$

ϵ is equal to 0.5 for a star polymer.³⁵ The viscosity branching factor can be calculated with the intrinsic viscosity ratio of the star polymer ($[\eta]_s$) and its linear analogue ($[\eta]_l$) with the same molar mass (Equation 4).

$$g' = \frac{[\eta]_s}{[\eta]_l} \quad (4)$$

The intrinsic viscosity can be measured directly by the viscometer of the HT-SEC. Therefore, we used this approach to determine the number of arms of each polymer and compare it with the expected values.

Nevertheless, PEs synthesized by a radical process are low-density polyethylenes (LDPE). LDPEs are already branched structures and contain both long and short-chain branching (LCB and SCB, respectively). This branching nature adds to the difficulty in characterizing the star nature of our polymers. Under our conditions, the formed PE chains are much less branched than the conventional LDPE as the softer

polymerization conditions employed here (80 bar, 70 °C) induces less transfer reactions.¹⁴⁻¹⁷

To calculate the number of arms when CTA-S3 and CTA-S4 were employed, the polymers synthesized in the presence of CTA-S1 and CTA-S2 were used as linear equivalents in Equation 4. The number of arms calculated for PE synthesized in the presence of CTA-S3 was on average 2.8 after 3 h of reaction. For PE synthesized in the presence of CTA-S4, the average value was 4.1 after 3h of reaction. The consistency observed with the expected values of 3 and 4 when CTA-S3 and CTA-S4 are used, respectively, showed that the targeted 3- and 4-armed star PEs were obtained.

Eventually, the PEs synthesized in the presence of the different CTAs present the advantage of having ester functions that can be selectively cleaved to retrieve and assess the homogeneity of PE arms.

The PEs obtained after 6 hours of polymerization were hydrolyzed with *t*BuOK and subsequently analyzed by SEC (Figure 7). Figure 7a shows that, as expected, this treatment is not affecting the molar mass of the PE obtained with CTA-S1. On the other hand, for the PE synthesized in the presence of CTA-S2, CTA-S3, and CTA-S4, the molar mass distributions shifted toward lower molar masses (Figure 7, b-d). As expected, the shift is more pronounced when the number of arms in the targeted star polymer increases. As the [iodine]:[AIBN] ratio was kept the same for all the experiments, the targeted molar masses of each PE arm are identical after the same polymerization time. This is confirmed by the overlay of the molar mass distributions in Figure 7e. Moreover, using a PE calibration, $M_n(\text{SEC})$ values of 2150, 1950, 2000, 1950 g mol^{-1} (\mathcal{D} of 1.92, 1.97, 2.19, 2.29, respectively) were measured after treatment of PE obtained with CTA-S1, CTA-S2, CTA-S3, and CTA-S4, respectively. All these data confirmed the successful synthesis of star PEs.

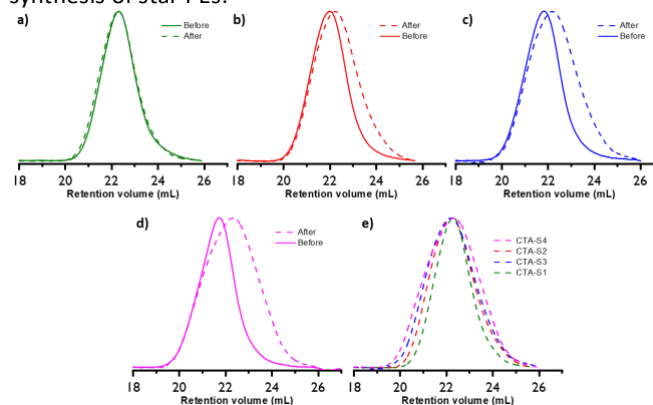


Figure 7. Molar mass distributions of PE before and after hydrolysis by *t*BuOK of PE obtained in the presence of a) CTA-S1, b) CTA-S2, c) CTA-S3, and d) CTA-S4. e) Molar mass distributions comparison after hydrolysis.

4-arm star EVA copolymers. Considering the excellent control observed for the ITP of ethylene mediated by the CTA-S, we anticipated that iodine transfer copolymerization (ITCoP) of ethylene with VAc might be a powerful tool to produce star P(E-co-VAc). In the following, we examined the ITCoP of ethylene and VAc in the presence of CTA-S4. Copolymerizations were

carried out with 25 mL of VAc (replacing part of the solvent DMC, total volume 50 mL) at 80 bar of ethylene and 70 °C, with 50 mg of AIBN ([iodine]:[AIBN] = 3:1) to target a VAc content of 25 mol%. The kinetics of the corresponding experiments are presented in **Table 1**.

Table 1. ITCoPs of ethylene and VAc mediated by CTA-S4.^[a]

Run	Time (h)	Monomer cons. ^[b] (g)	M_n (theo.) ^[c] (g mol ⁻¹)	VAc content ^[d] (mol%)	M_n (NMR) ^[e] (g mol ⁻¹)	M_n (SEC) ^[f] (g mol ⁻¹)	\bar{D} ^[f]	T_m ^[g] (°C)	T_g ^[g] (°C)
1	1.5	2.7	12500	26	14500	14200	1.5	0.6	-30.6
2	3	5.9	27000	25	34300	22400	1.4	0.1	-29.3
3	6	11.7	51000	25	58500	36200	1.6	-1.7	-30.4

[a] AIBN (0.3 mmol), [iodine]:[AIBN] = 3:1 at 70 °C and 80 bar in 25 mL of DMC with 25 mL of VAc. [b] Monomer consumption = (mass of dried product) - (mass of AIBN) - (mass of CTA). [c] M_n (theo.) = (monomer cons. [g]) / (CTA [mol]) + M (CTA). [d] Calculated by ¹H NMR by comparing the CH₂ signals of the ethylene unit and the CH of the vinyl acetate unit. [e] Calculated by comparing the ¹H NMR signals of the EVA chain and the iodo chain-end. [f] Determined by THF-SEC with a PS calibration. [g] Determined by DSC.

Molar masses measured by ¹H NMR (**Figure 8a**) showed an excellent consistency with the expected values (*i.e.*, for run 3 in **Table 1**, M_n (NMR) = 58500 g mol⁻¹ and M_n (theo.) = 51000 g mol⁻¹). The polymerization system yields copolymers with unimodal molar mass distributions shifting toward higher molar masses for higher monomer consumptions (**Figure 8b**). As already discussed,¹⁹ M_n (SEC) and \bar{D} for the P(E-co-VAc) should be taken with caution. Indeed, different arms and monomer contents might lead to different elution behavior during the SEC experiment. We thus considered NMR spectroscopy being more reliable for a quantitative comparison of the M_n values of the copolymers. Still, good agreement was observed between M_n (SEC), M_n (NMR), and M_n (theo.) (**Table 1**). In conclusion, the ITCoP of ethylene and VAc mediated by CTA-S4 shows a good control. The star copolymers exhibit glass transition and melting temperatures comparable to those obtained previously for linear analogue with the same VAc content.¹⁹

The EVA star polymers are more challenging to characterize by hydrolysis similarly to their PE analogues since the hydrolysis of the EVA core resulted in the hydrolysis of VAc units, complicating the chromatograms comparisons.

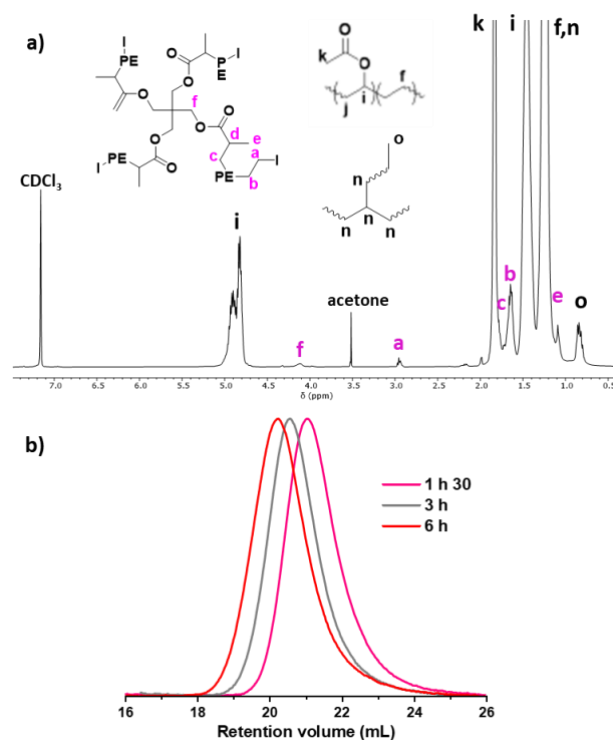


Figure 8. Molar mass distributions of P(E-co-VAc) obtained during the ITCoP of ethylene and VAc mediated by CTA-S4 (runs 4-6) with a VAc content of 25 mol%.

Conclusions

In conclusion, successful ITPs of ethylene were conducted with CTAS1-S4. In each cases a good control over the polymerization was shown and the final PE structures analyzed by ¹H NMR matched the expected ones. This was confirmed by analyzing the cleaved arms in the three and four-arm structures. The star nature of the PE obtained when CTA-S3 and CTA-S4 were used to mediate ITP was further shown by intrinsic viscosity measurements allowing to calculate a number of arms that is

consistent with the expected one. These good results prompted us to investigate the synthesis of EVA stars by successfully conducting ethylene and vinyl acetate ITPcoP.

Acknowledgements

F.B. acknowledges the French Ministère de l'Enseignement Supérieur de la Recherche et de l'Innovation (MESRI) for funding.

Conflicts of interest

There are no conflicts to declare.

Notes and references

- J. M. Ren, T. G. McKenzie, Q. Fu, E. H. H. Wong, J. Xu, Z. An, S. Shanmugam, T. P. Davis, C. Boyer and G. G. Qiao, *Chem. Rev.*, 2016, **116**, 6743-6836.
- A. Blencowe, J. F. Tan, T. K. Goh and G. G. Qiao, *Polymer*, 2009, **50**, 5-32.
- D. Fournier, R. Hoogenboom and U. S. Schubert, *Chem. Soc. Rev.*, 2007, **36**, 1369.
- J. Kim, H. Y. Jung and M. J. Park, *Macromolecules*, 2020, **53**, 746-763.
- G. Polymeropoulos, G. Zapsas, K. Ntetsikas, P. Bilalis, Y. Gnanou and N. Hadjichristidis, *Macromolecules*, 2017, **50**, 1253-1290.
- N. Hadjichristidis, M. Pitsikalis, S. Pispas and H. Iatrou, *Chem. Rev.*, 2001, **101**, 3747-3792.
- T. Tsoukatos and N. Hadjichristidis, 2002, **40**, 2575-2582.
- Y. Zhang, H. Li, Z. Xu, W. Bu, C. Liu, J.-Y. Dong and Y. Hu, *Polym. Chem.*, 2014, **5**, 3963-3967.
- D. Khedaioui, B. Burcher, D. Gajan, D. Montarnal, F. D'Agosto and C. Boisson, *Polym. Chem.*, 2020, **11**, 3884-3891.
- Y. Xue, S.-S. Zhang, K. Cui, J. Huang, Q.-L. Zhao, P. Lan, S.-K. Cao and Z. Ma, *RSC Adv.*, 2015, **5**, 7090-7097.
- K. Zhang, Z. Ye and R. Subramanian, *Macromolecules*, 2009, **42**, 2313-2316.
- P. Liu, E. Landry, Z. Ye, H. Joly, W.-J. Wang and B.-G. Li, *Macromolecules*, 2011, **44**, 4125-4139.
- X. Xia, Z. Ye, S. Morgan and J. Lu, *Macromolecules*, 2010, **43**, 4889-4901.
- C. Dommanget, F. D'Agosto and V. Monteil, *Angew. Chem. Int. Ind.*, 2014, **53**, 6683-6686.
- A. Wolpers, C. Bergerbit, B. Ebeling, F. D'Agosto and V. Monteil, *Angew. Chem. Int. Ind.*, 2019, **58**, 14295-14302.
- Y. Nakamura, B. Ebeling, A. Wolpers, V. Monteil, F. D'Agosto and S. Yamago, *Angew. Chem. Int. Ind.*, 2018, **57**, 305-309.
- A. Wolpers, F. Baffie, L. Verrieux, L. Perrin, V. Monteil and F. D'Agosto, *Angew. Chem. Int. Ind.*, 2020, **59**, 19304-19310.
- A. Wolpers, F. Baffie, V. Monteil and F. D'Agosto, *Macromol. Rapid Commun.*, 2021, **42**, 2100270.
- F. Baffie, M. Lansalot, V. Monteil and F. D'Agosto, *Polym. Chem.*, 2022, **13**, 2469-2476.
- A. Kermagoret, A. Debuigne, C. Jérôme and C. Detrembleur, *Nat. Chem.*, 2014, **6**, 179-187.
- J. Demarteau, A. Kermagoret, C. Jérôme, C. Detrembleur and A. Debuigne, in *Controlled Radical Polymerization: Materials*, American Chemical Society, 2015, vol. 1188, pp. 47-61.
- J. Demarteau, P. B. V. Scholten, A. Kermagoret, J. De Winter, M. A. R. Meier, V. Monteil, A. Debuigne and C. Detrembleur, *Macromolecules*, 2019, **52**, 9053-9063.
- L. Lei, M. Tanishima, A. Goto and H. Kaji, *Polymers*, 2014, **6**, 860-872.
- M. Tanishima, A. Goto, L. Lei, A. Ohtsuki, H. Kaji, A. Nomura, Y. Tsujii, Y. Yamaguchi, H. Komatsu and M. Miyamoto, *Polymers*, 2014, **6**, 311-326.
- Y. Liu and Z. Fan, *Designed Monomers and Polymers*, 2015, **18**, 251-261.
- J. Bernard, A. Favier, L. Zhang, A. Nilasaroya, T. P. Davis, C. Barner-Kowollik and M. H. Stenzel, *Macromolecules*, 2005, **38**, 5475-5484.
- H. Shimamura, T. Sunazuka, T. Izuhara, T. Hirose, K. Shiomi and S. Ōmura, *Organic Letters*, 2007, **9**, 65-67.
- V. Morozova, J. Skotnitzki, K. Moriya, K. Karaghiosoff and P. Knochel, *Angew. Chem. Int. Ind.*, 2018, **57**, 5516-5519.
- M. Guerre, G. Lopez, T. Soulestin, C. Totée, B. Améduri, G. Silly and V. Ladmiraal, *Macromol. Chem. Phys.*, 2016, **217**, 2275-2285.
- A. S. Kulkarni and G. Beaucage, *J. Polym. Sci. Part B Polym. Phys.*, 2006, **44**, 1395-1405.
- M. Gaborieau and P. Castignolles, *Analytical and Bioanalytical Chemistry*, 2011, **399**, 1413-1423.
- P. Liu, W. Liu, W.-J. Wang, B.-G. Li and S. Zhu, *Macromolecular Reaction Engineering*, 2017, **11**, 1600012.
- B. H. Zimm and W. H. Stockmayer, *The Journal of Chemical Physics*, 1949, **17**, 1301-1314.
- P. J. Flory and T. G. Fox, *J. Am. Chem. Soc.*, 1951, **73**, 1904-1908.
- W.-J. Wang, S. Kharchenko, K. Migler and S. Zhu, *Polymer*, 2004, **45**, 6495-6505.

